

# Synergistic effects of climate-related variables suggest future physiological impairment in a top oceanic predator

Rui Rosa<sup>1</sup> and Brad A. Seibel

Department of Biological Sciences, University of Rhode Island, 100 Flaggy Road, Kingston, RI 02881

Edited by George N. Somero, Stanford University, Pacific Grove, CA, and approved October 27, 2008 (received for review July 16, 2008)

**By the end of this century, anthropogenic carbon dioxide (CO<sub>2</sub>) emissions are expected to decrease the surface ocean pH by as much as 0.3 unit. At the same time, the ocean is expected to warm with an associated expansion of the oxygen minimum layer (OML). Thus, there is a growing demand to understand the response of the marine biota to these global changes. We show that ocean acidification will substantially depress metabolic rates (31%) and activity levels (45%) in the jumbo squid, *Dosidicus gigas*, a top predator in the Eastern Pacific. This effect is exacerbated by high temperature. Reduced aerobic and locomotory scope in warm, high-CO<sub>2</sub> surface waters will presumably impair predator-prey interactions with cascading consequences for growth, reproduction, and survival. Moreover, as the OML shoals, squids will have to retreat to these shallower, less hospitable, waters at night to feed and repay any oxygen debt that accumulates during their diel vertical migration into the OML. Thus, we demonstrate that, in the absence of adaptation or horizontal migration, the synergism between ocean acidification, global warming, and expanding hypoxia will compress the habitable depth range of the species. These interactions may ultimately define the long-term fate of this commercially and ecologically important predator.**

global warming | hypoxia | jumbo or Humboldt squid | ocean acidification | oxygen minimum layer

Atmospheric carbon dioxide [CO<sub>2</sub>]<sub>atm</sub> has increased from preindustrial levels of 280 ppm to >380 ppm today (1) and is expected to rise to 730–1020 ppm by the year 2100 [Coupled Climate–Carbon Cycle Model Intercomparison Project, C<sup>4</sup>MIP, Intergovernmental Panel on Climate Change (2)]. Almost half of the anthropogenic CO<sub>2</sub> released between 1800 and 1994 is now stored in the oceans (3), and ≈30% of recent emissions have been taken up by the ocean to date (4). Carbon dioxide reacts with seawater, resulting in a net increase in the concentration of H<sup>+</sup> (lowered pH) and a decrease in the carbonate ion (CO<sub>3</sub><sup>2-</sup>) concentration. This process, termed ocean acidification (5), is projected to decrease the pH of surface waters between 0.14 and 0.35 unit by the end of the 21st century (2). These future changes in the ocean's chemistry pose a serious problem for key marine organisms with CaCO<sub>3</sub> skeletons, such as corals and some plankton (6, 7). However, elevated CO<sub>2</sub> also has more broad detrimental effects on the survival, growth, and respiratory physiology of marine animals (8–10), although most of these experiments were not undertaken with ocean acidification in mind and used unrealistically high CO<sub>2</sub> levels. Thus, the effects of environmentally relevant pH reductions on noncalcifying marine biota are still poorly understood (7). At the same time, global ocean temperature has risen over the past few decades by 0.1°C from the surface to a depth of 700 m (11), causing, among other things, an expansion of the oceanic oxygen minimum layer (12). Additional warming and encroaching hypoxia in the coming century will also influence physiological processes (13–15) and may drive, at the community level, profound changes to trophic interactions (16), diversity, and biogeography (13, 17).

The synergistic effects of elevated CO<sub>2</sub>, hypoxia and temperature, are, to date, completely unexplored.

The jumbo squid, *Dosidicus gigas*, is a large pelagic top predator endemic to the Eastern Tropical Pacific (ETP), where temperature and oxygen are already near the upper and lower extremes, respectively, found in the oceans and where climate changes are expected to be pronounced (2). *D. gigas* reaches >2 m in total length and 50 kg in mass. Over the last few years, it has greatly extended its tropical/subtropical range as far north as Canada and Alaska, where it is now exerting a significant top-down control on commercial fish stocks (18). Like other ommastrephid squids, *D. gigas* displays a high oxygen demand that reflects high activity levels dictated by the pelagic environment and low efficiency of jet propulsion relative to other forms of locomotion (19). The metabolic capacity of these muscular squids is surprising considering the limitations of their respiratory systems. Their blood has low oxygen-carrying capacity, relative to similarly active fishes, because of viscosity-related constraints associated with an extracellular respiratory protein. In fact, they use all of the oxygen carried in the blood on each cycle through the body, even at rest, leaving no venous oxygen reserve. Furthermore, blood-oxygen binding in most active squids is highly pH sensitive (supporting information (SI) Table S1), a property that facilitates oxygen release to demanding tissues, but presumably interferes with oxygen extraction from hypoxic or CO<sub>2</sub>-rich seawater. Consequently, these organisms are thought to live chronically “on the edge of oxygen limitation” (20) and are not well poised to adapt to future environmental changes that influence oxygen supply and demand. Jumbo squids are thus expected to be particularly vulnerable to ocean acidification, global warming, and hypoxia. Surprisingly, *D. gigas* undergoes diel vertical migrations into zones of pronounced hypoxia at mesopelagic depths (21), known as oxygen minimum layers (OML).

To evaluate the effects of rapidly changing environmental parameters on the metabolic physiology of *D. gigas*, we exposed the jumbo squids to short-term (<24 h) elevations in CO<sub>2</sub>, equivalent to pessimistic predictions for the year 2100 (0.1% CO<sub>2</sub>, ≈1000 ppm; Δ pH = 0.3), while varying temperature and oxygen levels to match the conditions currently found at their night and daytime distributions (20°–25°C, 21% O<sub>2</sub> and 10°C, 1% O<sub>2</sub>, respectively).

Author contributions: R.R. and B.A.S. designed research; R.R. performed research; and R.R. and B.A.S. analyzed data and wrote the paper.

The authors declare no conflict of interest.

This article is a PNAS Direct Submission.

<sup>1</sup>To whom correspondence should be sent at the present address: Laboratório Marítimo da Guia, Centro de Oceanografia, Faculdade de Ciências da Universidade de Lisboa, Av. Nossa Senhora do Cabo, 939, 2750–374 Cascais, Portugal. E-mail: rrosa@fc.ul.pt.

This article contains supporting information online at [www.pnas.org/cgi/content/full/0806886105/DCSupplemental](http://www.pnas.org/cgi/content/full/0806886105/DCSupplemental).

© 2008 by The National Academy of Sciences of the USA

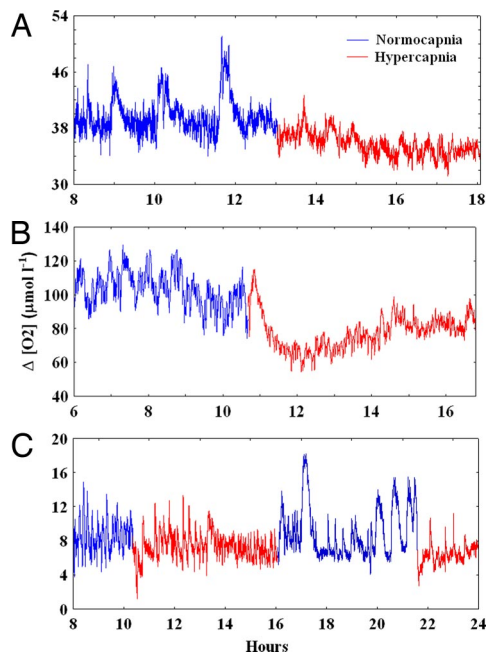


**Fig. 1.** Rhythmic sinusoidal oscillations of oxygen consumption in *Dosidicus gigas*. (A) An 8.03-g squid at 25°C. (B) A 21.93-g squid at 20°C. (C) A 2.23-g squid at 10°C. Rates are expressed as differences between the oxygen levels ( $\mu\text{mol liter}^{-1}$ ) recorded at the entrance and the exit of the chamber and oscillations reflect periodic activity peaks as indicated by recorded rates of mantle muscle contraction. Some specimens were exposed to two cycles of  $\text{CO}_2$  treatment (e.g., in C) to exclude the possibility that the observed trends in oxygen consumption were not driven by decreasing stress or food deprivation after placement in the chamber.

## Results and Discussion

All animals displayed a distinct periodicity of oxygen consumption rates (Fig. 1). Video analysis confirmed that the cycles, referred to here as “active cycles,” correlated with activity levels as indicated by rates of mantle contraction for jet propulsion. The occurrence of such activity peaks enabled us to quantify what we define as the maximal (MaxMR), active (AMR), routine (RMR), and inactive metabolic rates (IMR) and the mean number of active cycles per hour. These designations are based on the highest recorded rate (MRM), the average of rates expressed during peaks in the active cycles that were 20% higher (AMR) and 15% lower (IMR) than the average for the entire run (RMR) (see *Materials and Methods* for details). The percentages chosen to designate AMR and IMR are based on levels that approximated continuous activity and apparent inactivity (modest ventilatory movements only) in the video observations. Thus, IMR is, we believe, a reasonable approximation of a standard metabolic rate.

The jumbo squids displayed oxygen consumption rates that are among the highest in the oceans (Fig. 2). The squid’s lowest rates of mass-specific metabolism are higher than those of top vertebrate predators of equivalent size, including sharks and tunas (Fig. 2B). However, under hypoxic conditions (Fig. 3B), IMR decreased by  $\approx 80\%$  from an average of 7.0 (control) to  $1.4 \mu\text{mol O}_2 \text{ g}^{-1} \text{ h}^{-1}$  (Fig. 3A). A concomitant enhancement of glycolysis, as indicated by an accumulation of octopine (Fig. S1), compensates for only a small fraction ( $<10\%$ ) of the energy deficit that resulted from the decline of aerobic ATP synthesis. In the absence of reduced oxygen demand, we calculate that the rate of ventilation that would be required to meet oxygen demand, assuming complete extraction of oxygen from the respiratory stream, increases dramatically with depth (Fig. 3C). Because ventilation and locomotion are tied via contraction of the large

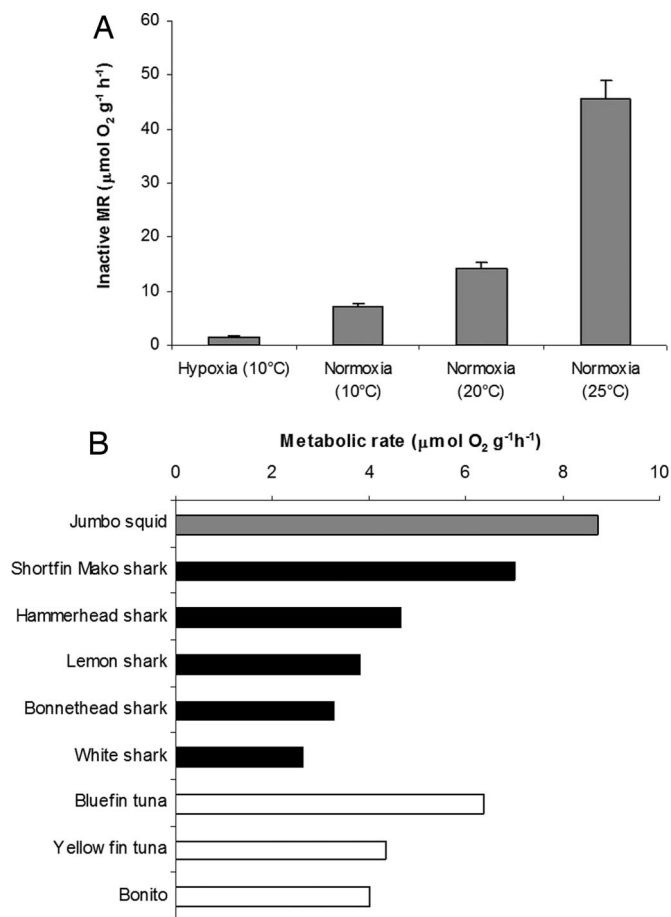


**Fig. 2.** Inactive mass-specific oxygen consumption rates (IMR,  $\mu\text{mol O}_2 \text{ g}^{-1} \text{ h}^{-1}$ ) in jumbo squid, *Dosidicus gigas*. (A) Effect of temperature and oxygen (hypoxia, 1%  $\text{O}_2$ ; normoxia, 21%  $\text{O}_2$ ) on IMR. Values are means  $\pm$  SE (more details in supporting online material, Table S2). (B) Comparison of estimated IMR ( $\mu\text{mol O}_2 \text{ g}^{-1} \text{ h}^{-1}$ ) of jumbo squid and the standard metabolic rate (calculated by extrapolating to zero speed) of other top predators in the Eastern Tropical Pacific (ETP) (sources for shark and tuna data are available in Table S3). Rates were estimated for 1-kg animals and standardized to 20°C, assuming a  $Q_{10}$  of 2 and a scaling coefficient of  $-0.25$  for fishes. For *D. gigas*, the extrapolation to bigger size was based on the common tendency for isometric metabolic scaling ( $\text{IMR} = aM^{0.04}$  at 20°C, Table S2) in muscular squids (22).

muscular mantle (23), ventilation is a very costly part of the energy budget in squids. Excess ventilation during hypoxic exposure would drive oxygen demand up in a positive feedback loop that would presumably prohibit the maintenance of routine aerobic metabolic rates in the oxygen minimum layer. Thus, whereas the OML restricts the depth distribution of competing vertebrate predators to the upper surface layers because of their more limited hypoxia tolerance (ref. 24, Fig. 3B), *D. gigas* circumvents similar restrictions via metabolic suppression and spends the daytime in deep, cold, and oxygen-depleted waters (Fig. 3).

The profound hypoxia-induced metabolic suppression (Figs. 2A and 3A) extends the squid’s survival time in the OML, by conserving the finite stores of fermentable substrate, minimizing cytotoxicity and limiting the oxygen debt that must be repaid upon return to oxygen-replete surface waters. Oxygen debt typically includes the costs of replenishing substrate stores and removing toxic end products of anaerobic metabolism. Payment of such debts entails a substantial increase in oxygen consumption (25). Although the oxygen debt incurred by *D. gigas* is minimized by the substantial suppression of ATP-consuming

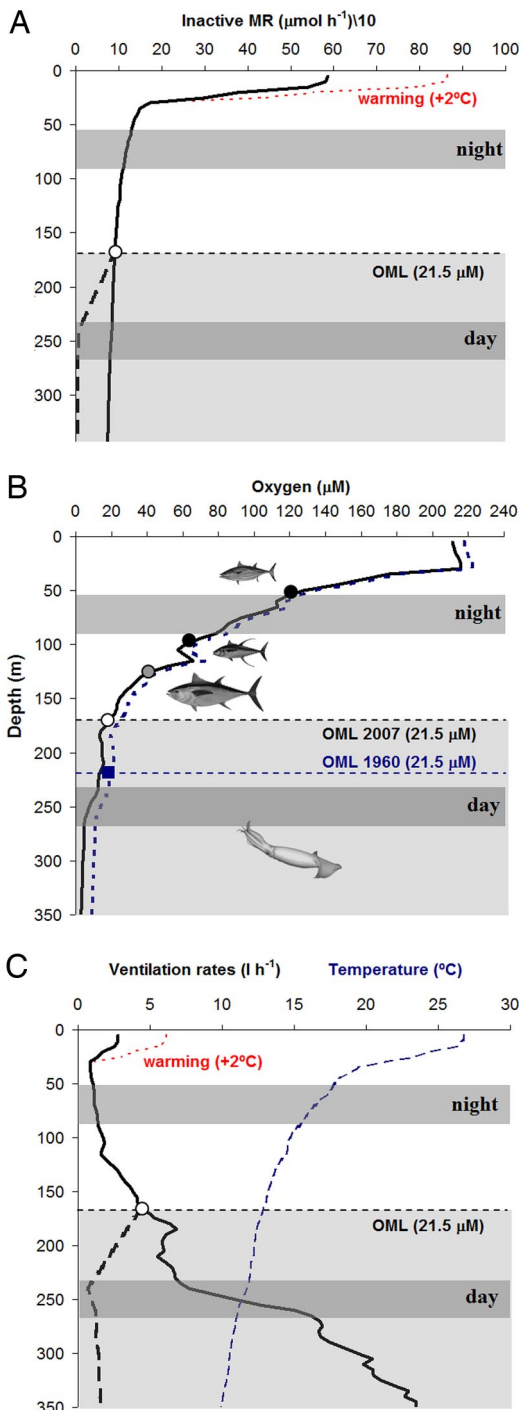


**Fig. 3.** Metabolic physiology and vertical ecology of *Dosidicus gigas*. (A) Projected inactive metabolic rates (10-g animal,  $\mu\text{mol O}_2 \text{h}^{-1}$ , black solid line) as a function of depth in the Gulf of California. The thick black dashed line reflects the expected metabolic depression after reaching the squid's critical oxygen partial pressure,  $P_c$  ( $21.5 \mu\text{M}$ , open circle, (21). The thin red dashed line shows the increase in metabolic rate because of expected ocean surface warming ( $2^\circ\text{C}$ ) in the Eastern Tropical Pacific (ETP) (2). Gray bars represent the main depth range occupied by *D. gigas* during daytime ( $\approx 250$  m) and nighttime ( $\approx 70$  m) periods (21). (B) Depth-related changes in oxygen levels ( $\text{ml liter}^{-1}$ , black solid line) and hypoxic thresholds (critical  $\text{PO}_2$ ,  $P_c$ , symbols) of several ETP top predators. Note that the partial pressure of oxygen (i.e., the actual driver of oxygen flux into the organism) at a given concentration will vary with temperature. Open circle, jumbo squid's  $P_c$ ; light gray circle, bigeye tuna (*Thunnus obesus*); deeper black circle, yellowfin tuna (*Thunnus albacares*); and shallower black circle, skipjack tuna (*Katsuwonus pelamis*). Sources for tuna data are available in [Table S4](#). The thick blue dashed line

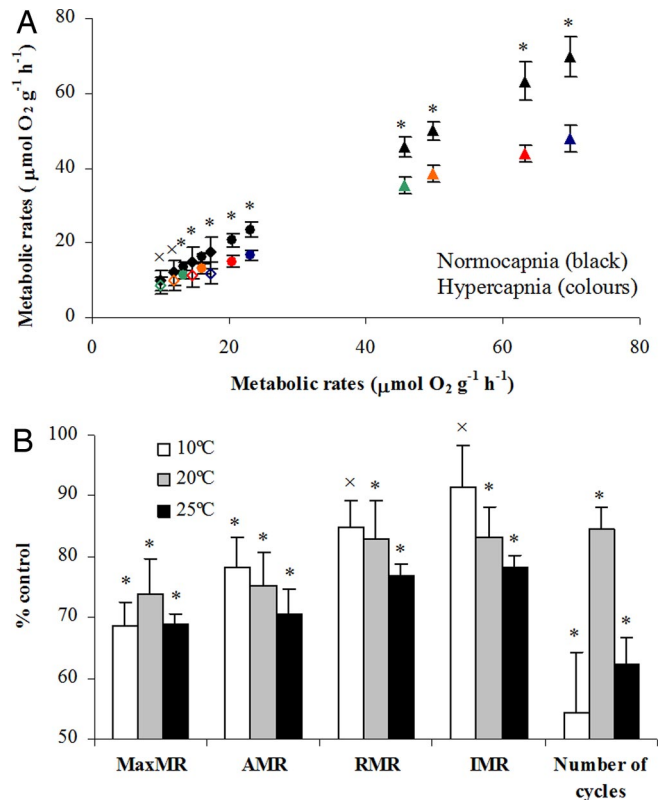


**Fig. 4.** Effect of hypercapnia in the metabolic physiology of jumbo squid, *Dosidicus gigas*. (A) Mean oxygen consumption rates ( $\pm$  SE;  $\mu\text{mol O}_2 \text{g}^{-1} \text{h}^{-1}$ ) under control (black symbols) and hypercapnic treatments at inactive (IMR), routine (RMR), active (AMR), and maximum (MRM) levels (green, orange, red, and blue symbols, respectively). Oxygen consumption rates under control conditions are plotted against themselves and against rates of those same individuals under elevated ( $0.1\%$ )  $\text{CO}_2$ . Open diamonds,  $10^\circ\text{C}$ ; solid circles,  $20^\circ\text{C}$ ; solid triangles,  $25^\circ\text{C}$  (plots with individual runs are available in supporting online material). (B) Oxygen consumption rates and activity levels (number of active cycles per hour) under high  $\text{CO}_2$  expressed as a percentage of the control values at the three different temperatures. \*, significant differences (paired  $t$  test,  $P < 0.05$ );  $\times$ , nonsignificant differences (paired  $t$  test,  $P > 0.05$ )

activities, it is probably not negligible and will add to the already high metabolic costs associated with warm surface temperatures.

Under the elevated  $\text{CO}_2$  conditions predicted for the end of this century, the squid's oxygen demand was significantly reduced (Figs. 1 and 4, and [Fig. S2](#)). At  $25^\circ\text{C}$ , MaxMR decreased, on average, from  $70$  to  $48 \mu\text{mol O}_2 \text{g}^{-1} \text{h}^{-1}$  ( $P < 0.05$ ; [Fig. 4A](#)), which represented a reduction of  $31\%$  ([Fig. 4B](#)). Similar  $\text{CO}_2$ -induced decreases in MaxMR were attained at  $10^\circ$  and  $20^\circ\text{C}$  ( $P < 0.05$ ; [Fig. 4A](#) and [B](#)). Significant reductions were also observed for all of the other measured rates and temperatures, with the

represents the predicted oxygen levels in 1960. These estimates were based on a decrease in oxygen of  $0.13 \mu\text{mol kg}^{-1} \text{year}^{-1}$  from 1960 to 2008 in the ETP pelagic ecosystem (12). The expansion of the oxygen-minimum layer (OML) drives the hypoxic threshold to shallower depths (illustrated by the change in the squid's  $P_c$ , blue square and open circle), causing a more compressed epipelagic habitat. The bathymetric difference between the past and the present  $21.5\text{-}\mu\text{M}$  ( $\approx 0.5 \text{ ml liter}^{-1}$ ) oxyline is  $65$  m. (C) Temperature ( $^\circ\text{C}$ , thin blue dashed line) and projected ventilation rates in *D. gigas* (10-g animal) as a function of depth. Ventilation rate ( $\text{l h}^{-1}$ , black solid line) equals the water volume from which all  $\text{O}_2$  must be extracted per hour to support standard metabolism. The thick black dashed line reflects the expected ventilation rate reduction after reaching the squid's  $P_c$ . The thin red dashed line shows the increase in ventilation rate because of the ocean surface warming.

exceptions of RMR and IMR at 10°C (crosses in Fig. 4). The number of activity cycles per hour was also significantly reduced between 55 and 84% ( $P < 0.05$ ; Fig. 4B).

Although the OML environment is characterized by both hypoxia and high CO<sub>2</sub> levels (26), our results indicate that the effect of oxygen availability on the squid's metabolic rate overwhelms the more subtle CO<sub>2</sub> effect while at its cold, hypoxic daytime habitat depth. Low pH and high CO<sub>2</sub> are common triggers of metabolic depression (27), but they do not cause a substantial metabolic depression in *D. gigas* while in the OML (Fig. 4B). However, at warmer temperatures, carbon dioxide becomes an important influence on *D. gigas*' metabolic rate.

The effect of temperature on aerobic metabolism, expressed as a temperature coefficient ( $Q_{10}$ ), changed dramatically across the temperature range studied (Fig. 2A). Coefficients of  $\approx 2$  and 7 were measured for IMR between 10°–20°C and 20°–25°C, respectively. While the former is within the normal range of temperature effects on metabolism in most ectotherms (28), the unusually high  $Q_{10}$  values over the 20°–25°C range may indicate that temperatures >20°C are not optimal for these highly aerobic animals. Field data with satellite-linked pop-up archival transmitting tags in the Sea of Cortez support this contention. Gilly and collaborators (21) reported that *D. gigas* spends <10% of its time at temperatures >20°C, while Davis and collaborators (29) reported that the cumulative probability of a squid making a deep dive was reduced to only a few minutes at temperatures >22°C. In other words, excursions into warm surface waters were often terminated by rapid deep dives to cooler waters that are thought to provide thermal relief.

By the end of the 21st century, the ETP is expected to warm, between 2° and 3°C because of weakening tropical circulations (2), and seawater pH will decline by as much as 0.3 unit. Warmer temperatures will elevate metabolism and require enhanced performance from a constrained oxygen transport system that will be impaired, especially at high temperatures, by ocean acidification (20) (projections in Figs. 3A and C and 4). Thus warming and acidification may cause ventilatory and circulatory stress that restricts the squid's aerobic scope and impairs swimming activity. Together these variables may reduce the animal's ability to respond to external stimuli, leaving it more vulnerable to its main predators. Moreover, if the OML continues to expand vertically in the ETP (12), *D. gigas* will have to retreat to even shallower waters at night to repay any accumulated oxygen debt and to hunt. Thus, ocean acidification and warming may create a ceiling that precludes these squids from entering near-surface waters, while the expanding hypoxic zone may elevate the floor below which they cannot penetrate during their night-time recovery from hypoxia. The synergistic effect of these three climate-related variables may be to vertically compress the habitable night-time depth range of the species (Fig. 3B).

This hypothesized habitat compression (24) may alter the squid's behavioral and feeding ecology with cascading effects on growth and reproduction. Jumbo squids are an important commercial fishery throughout the ETP and are important components in the diets of birds, fishes, and mammals there (29). While

poorly constrained at present, we expect that the capacity for adaptation to climate change in epipelagic squids is limited, given the very restricted environmental conditions under which oxygen transport is sufficient to meet very high rates of oxygen demand.

## Materials and Methods

Jumbo squids, *D. gigas* (1.2–50.8 g of total weight), were collected in Santa Rosalia (27°N, 112°W) and Guaymas (27°N, 111°W) basins in the Gulf of California (aboard RV *New Horizon*, Scripps Institution) in May and June 2006 and June 2007 and in the Eastern Tropical Pacific (ETP1, 13°N, 104°W; ETP2, 8.5°N, 90°W; aboard RV *Seward Johnson*, Harbor Branch) in October and November 2007. Specimens were captured during the night, at the surface, by using a hand-held dip net (area  $\approx 40$  cm<sup>2</sup>), and immediately transferred to 10°C or 20°C aerated seawater aquaria on board ship where they were maintained up to 12 h before placement in a respiratory chamber. A total of 86 specimens were used.

Specimens were placed in a flow-through respirometer (270 ml volume, Loligo Systems), where they were allowed to acclimate for 8–12 h before measurements of aerobic metabolism began. Respirometers were immersed in a large thermostated water bath. Filtered (0.2  $\mu$ m) and treated (50 mg liter<sup>-1</sup> streptomycin) seawater was pumped from a water-jacketed gas-equilibration column through the respirometers at a constant flow rate of 140 ml min<sup>-1</sup>. The water in the column was bubbled continuously with humidified certified mixtures of air to maintain incoming water at normal (21% O<sub>2</sub>) or low PO<sub>2</sub> (certified gas mixture with 1% O<sub>2</sub>) for the hypoxia experiments and high (certified gas mixture with 0.1% CO<sub>2</sub>) or normal PCO<sub>2</sub> (0.03% CO<sub>2</sub>) for the CO<sub>2</sub> experiments. The pH of the afferent water was measured (Orion model 720A+ meter, flow-thru pH, Microelectrodes Inc.) to ensure that a constant CO<sub>2</sub> level had been reached. CO<sub>2</sub> treatment resulted in a 0.3 unit pH decrease (normocapnia pH 7.93  $\pm$  0.05; hypercapnia pH 7.62  $\pm$  0.08). Oxygen concentrations were recorded at the entrance and the exit of each chamber with two Clarke-type O<sub>2</sub> electrodes connected to a Strathkelvin Instruments 928 Oxygen Interface. The system was calibrated using air- and nitrogen-saturated seawater and checked for electrode drift and for microbial oxygen consumption before and after each trial. All experiments were carried out in darkness and at atmospheric pressure.

All animals showed a distinct periodicity to the oxygen consumption rates on time intervals of  $\approx 20$  min, and video analysis confirmed that the cycles correlated with activity levels as indicated by rates of mantle contraction for jet propulsion. During periods of activity, metabolic rates (MR) were  $\approx 20\%$  higher than the routine levels (RMR, average rate for the entire experiment). Thus, the AMR was quantified by averaging the rates for all peaks >20% higher than the RMR. IMR were quantified by averaging peaks of the experiment that were 15% lower than the routine rate. These rates correlated with periods of apparent inactivity in the chambers. MaxMR were quantified as the highest rate achieved during a given treatment and were typically 35–100% higher than the RMR.

Note that pelagic predators such as *D. gigas* rarely stop swimming in nature and that we did not quantify locomotion continuously for any experiment in its entirety. Thus, while our inactive metabolic rates do not necessarily meet the criteria set for "standard" metabolic rates in mammalian and other model organisms, we feel that they are a reasonable approximation of a standard metabolic rate.

**ACKNOWLEDGMENTS.** We thank the captains and the crews of the RV *New Horizon* and the RV *Seward Johnson*. Lloyd Trueblood, Sarah Marnell, Leanne Birden, Al Nyack, Amy Maas, and Rachel Wigton assisted in specimen collection at sea. This research was supported by the National Science Foundation (OCE-0526493 and OCE-0526545 to B.A.S.). The Portuguese Fundação para a Ciência e Tecnologia (SFRH/BPD/19396/2004) and Fundação Calouste Gulbenkian (ref. 78983) supported this study through postdoctoral grants to R.R.

- Petit JR, et al. (1999) Climate and atmospheric history of the past 420,000 years from the Vostok ice core, Antarctica. *Nature* 399:429–436.
- Meehl GA, et al. (2007) *Climate Change 2007: The Physical Science Basis. Contribution of Working Group I to the Fourth Assessment Report of the Intergovernmental Panel on Climate Change*, eds Solomon S, et al. (Cambridge Univ Press, Cambridge, UK), pp 747–845.
- Sabine CL, et al. (2004) The oceanic sink for anthropogenic CO<sub>2</sub>. *Science* 5682:367–371.
- Feely RA, et al. (2004) Impact of anthropogenic CO<sub>2</sub> on the CaCO<sub>3</sub> system in the oceans. *Science* 305:362–366.
- Caldeira K, Wickett ME (2003) Anthropogenic carbon and ocean pH. *Nature* 425:365.
- Orr JC, et al. (2005) Anthropogenic ocean acidification over the twenty-first century and its impact on calcifying organisms. *Nature* 437:681–686.

- Kleypas JA, et al. (2006) *Impacts of Ocean Acidification on Coral Reefs and Other Marine Calcifiers. A Guide for Future Research* (Report of a workshop held 18–20 April 2005, St Petersburg, FL, sponsored by NSF, NOAA, and the U.S. Geological Survey, 2006), pp 1–96.
- Seibel BA, Fabry VJ (2003) Marine biotic response to elevated carbon dioxide. *Adv Appl Biodivers Sci* 4:59–67.
- Pörtner HO, Langenbuch M, Reipschlag A (2004) Biological impact of elevated ocean CO<sub>2</sub> concentrations: lessons from animal physiology and earth history. *J Oceanogr* 60:705–718.
- Seibel BA, Walsh PJ (2001) Potential impacts of CO<sub>2</sub> injection on deep-sea biota. *Science* 294:319–320.
- Bindoff NL, et al. (2007) *Climate Change 2007: The Physical Science Basis. Contribution of Working Group I to the Fourth Assessment Report of the Intergovernmental Panel on Climate Change*, eds Solomon S, et al. (Cambridge Univ Press, Cambridge, UK), pp 385–432.

12. Stramma L, Johnson GC, Sprintall J, Mohrholz V (2008) Expanding oxygen-minimum zones in the tropical oceans. *Science* 320:655–658.
13. Somero GN (2005) Linking biogeography to physiology: evolutionary and acclimatory adjustments of thermal limits. *Front Zool* 2:1–9.
14. Tewksbury JJ, Huey RB, Deutsch CA (2008) Putting the heat on tropical animals. *Science* 320:1296–1297.
15. Childress JJ, Seibel BA (1998) Life at stable low oxygen levels: adaptations of animals to oceanic oxygen minimum layers. *J Exp Biol* 201:1223–1232.
16. Edwards M, Richardson AJ (2004) Impact of climate change on marine pelagic phenology and trophic mismatch. *Nature* 430:881–884.
17. Perry AL, Low PJ, Ellis JR, Reynolds JD (2005) Climate change and distribution shifts in marine fishes. *Science* 308:1912–1915.
18. Zeidberg LD, Robison BH (2007) Invasive range expansion by the Humboldt squid, *Dosidicus gigas*, in the eastern North Pacific. *Proc Natl Acad Sci USA* 104:12948–12950.
19. O'Dor RK, Webber DM (1986) The constraints on cephalopods: why squid aren't fish. *Can J Zool* 64:1591–1605.
20. Pörtner HO (2002) Environmental and functional limits to muscular exercise and body size in marine invertebrates athletes. *Comp Biochem Physiol A* 133:303–321.
21. Gilly WF, et al. (2006) Vertical and horizontal migrations by the jumbo squid *Dosidicus gigas* revealed by electronic tagging. *Mar Ecol Prog Ser* 324:1–17.
22. Seibel BA (2007) On the depth and scale of metabolic rate variation: scaling of oxygen consumption rates and enzymatic activity in the Class Cephalopoda (Mollusca). *J Exp Biol* 210:1–11.
23. Wells MJ (1990) Oxygen extraction and jet propulsion in cephalopods. *Can J Zool* 68:815–824.
24. Prince ED, Goodyear CP (2006) Hypoxia-based habitat compression of tropical pelagic fishes. *Fish Oceanogr* 15:451–464.
25. Lewis JM, et al. (2007) Responses to hypoxia and recovery: repayment of oxygen debt is not associated with compensatory protein synthesis in the Amazonian cichlid, *Astronotus ocellatus*. *J Exp Biol* 210:1935–1943.
26. Millero FJ, Deglera EA, O'Sullivan DW, Goyet C, Eiseidc G (1998) The carbon dioxide system in the Arabian Sea. *Deep-Sea Res II* 45:2225–2252.
27. Guppy M, Withers P (1999) Metabolic depression in animals: physiological perspectives and biochemical generalizations. *Biol Rev* 74:1–40.
28. Hochachka PW, Somero GN (2002) *Biochemical Adaptation: Mechanisms and Process in Physiological Evolution* (Oxford Univ Press, Oxford).
29. Davis RW, et al. (2007) Diving behavior of sperm whales in relation to behavior of a major prey species, the jumbo squid, in the Gulf of California, Mexico. *Mar Ecol Prog Ser* 333:291–302.